ELSEVIER

Mechanics of Materials 24 (1996) 43–57

MECHANICS OF MATERIALS

A new computational approach to crystal plasticity: fcc single crystal

Sia Nemat-Nasser *, Tomoo Okinaka

Center of Excellence for Advanced Materials, Department of Applied Mechanics and Engineering Sciences, University of California, San Diego, La Jolla, CA 92093-0411, USA

Received 6 May 1996

Abstract

An algorithm is proposed for the calculation of the finite deformation of fcc single crystals, using a rate-dependent slip model. The method also applies to bcc and hcp crystals. The history of the deformation is divided into three regimes, depending on the number of *active* slip systems, and a computational strategy is proposed for each regime. The proposed algorithm uses a combination of the forward-gradient and the plastic-predictor elastic-corrector methods. The efficiency and the accuracy of the proposed algorithm is demonstrated by comparing the results with those of the conventional method.

1. Introduction

The objective is to establish an efficient algorithm for the analysis of finite deformation of single crystals. The dynamic material response of a single crystal is evaluated incrementally, based on its elastoplastic constitutive relations which, in general, depend nonlinearly upon the current deformation and stress states of the crystal. Although fcc single crystals are considered in this work, the method also applies to bcc and hcp crystals. The rate-dependent slip theory of crystals is used, since most materials are rate sensitive.

The constitutive relations of single crystals based on rate-dependent slip theories have been discussed by many investigators; see Rice (1971), Hutchinson (1976), Hutchinson (1977), Pan and Rice (1983), Peirce et al. (1983), Asaro and Needleman (1985), Nemat-Nasser and Obata (1986), Rashid and Nemat-Nasser (1990), Zikry and Nemat-Nasser (1990), Rashid and Nemat-Nasser (1992), and Rashid et al. (1992). The approach that has generally been followed in the past studies, is based on the linearization of the nonlinear constitutive relations which are then evaluated using an implicit time integration technique. Nemat-Nasser and Obata (1986) established a self-consistent approach for polycrystals which is based on such a linearization of the constitutive relations of the corresponding single-crystal constituents, following the method proposed by Iwakuma and Nemat-Nasser (1984) for the rate-independent slip theories. Although the forward-gradient method (tangent-modulus method) is a useful approach, it leads to a stiff system of constitutive equations which require very small time increments in order to obtain the desired accuracy and stability

* Corresponding author.

PII S0167-6636(96)00020-8

in their numerical implementation. Rashid and Nemat-Nasser (1992) proposed an integration scheme to solve the rate-dependent planar double slip model, and simulated heterogeneous deformation in copper single crystals.

A semi-explicit and efficient finite deformation algorithm has been developed recently, and it has been applied to stiff phenomenological constitutive equations with considerable success; see Nemat-Nasser (1991), Nemat-Nasser (1992), Nemat-Nasser and Chung (1992), Nemat-Nasser and Li (1992), and Nemat-Nasser and Li (1994). The method exploits the physical fact that large deformations of metals are due to plastic flow with only a very small accompanying elastic contribution. Hence, in finite deformation problems, it is more efficient to first assume that the total deformation increment is due to plastic flow (plastic-predictor) and then correct the results to account for the accompanying elastic deformations (elastic-corrector). This predictor–corrector method has been successfully applied by Nemat-Nasser and coworkers to many large deformation problems, where large time increments have been used without impairing the required accuracy. With such time increments, the commonly used forward-gradient method looses both stability and accuracy due to the stiffness of the involved system of equations. The often-used radial-return method has been modified by Balendran and Nemat-Nasser (1994) for applications to phenomenological elastoplasticity models, based on the plastic-predictor concept.

An efficient algorithm for calculating the finite deformation of single crystals is proposed by using the physical fact exploited by Nemat-Nasser and coworkers. Unlike the phenomenological cases, in single crystals, the elastic contribution may not necessary be small when compared with the plastic one, unless five linearly independent slip systems are active. Hence, a different plastic-predictor/elastic-corrector method is applied, depending on the number of the active slip systems. When in certain stages of the deformation, the elastic contribution becomes important, then the forward-gradient method provides a better computational tool. This is the case when the active slip systems are changing rapidly, and new slip systems are becoming active. In general, the number of active slip systems is less than five at the initial yielding point of the material, and increases with time under a monotonic loading condition. The proposed algorithm consists of three different numerical calculation techniques: two new predictor–corrector techniques and the forward-gradient method. Large time increments can be used with the new predictor–corrector techniques. The proposed algorithm automatically selects a proper numerical calculation strategy without a need of interference by an operator.

In Section 2, the fundamental kinematics of finite deformation crystal plasticity and the elastoplastic constitutive relations for fcc single crystals are briefly discussed. The interdependency of resolved shear stresses is discussed in Section 3. In Section 4, a new algorithm is proposed for this class of crystals. The results of the numerical calculations are presented in Section 5, and are compared with the results of the forward-gradient method. Through this comparison, the accuracy and the efficiency of the proposed algorithm is discussed.

The following convention is used. The second order identity tensor is represented by **1**. A rectangular Cartesian coordinate system, whose axes coincide with the crystallographic axes in the initial lattice structure, is used throughout this work. Quantities **AB**, **Av**, and C: **A** have the following component representation: $(\mathbf{AB})_{ij} = \Sigma_{k=1}^{3} A_{ik}B_{kj}$, $(\mathbf{Av})_i = \Sigma_{k=1}^{3} A_{ik}v_k$, and $(\mathbf{C}:\mathbf{A})_{ij} = \Sigma_k = 1^3 \Sigma_{l=1}^{3} C_{ijkl}A_{kl}$. Also $\mathbf{a} \otimes \mathbf{b}$, $\langle \mathbf{A}, \mathbf{B} \rangle$, and tr[**A**] respectively denote the tensor product, the inner product, and the trace of the second order tensor. Their components are $(\mathbf{a} \otimes \mathbf{b})_{ij} = a_i b_j$, $\langle \mathbf{A}, \mathbf{B} \rangle = \Sigma_{i=1}^{3} \Sigma_{j=1}^{3} A_{ij}B_{ij}$, and $\mathrm{tr}[\mathbf{A}] = \Sigma_{i=1}^{3} A_{ii}$.

2. Fundamental kinematics and constitutive relations

2.1. Kinematics

The general kinematics of the elastic–plastic deformation of crystals at finite strains is given by Hill (1966), Rice (1971), Hill and Rice (1972), and developed by Havner (1973), Kroner and Teodosiu (1974), Rice (1975), Asaro (1979), Nemat-Nasser et al. (1981), and Hill and Havner (1982). Reviews are given by Nemat-Nasser (1983), Asaro (1983), and Havner (1992). In particular, Havner (1992) provides

a comprehensive account of the subject and cites many relevant references.

The total deformation gradient is defined by

$$\mathbf{F} = \frac{\partial \mathbf{x}}{\partial \mathbf{X}}, \tag{1a}$$

where $\mathbf{X}$ and $\mathbf{x}$ denote the reference and current particle positions, respectively. The formulation is based on the assumption that material deforms plastically by crystalline slip, while the lattice undergoes elastic deformation. Hence, the total deformation gradient, $\mathbf{F}$, can be divided into a non-plastic deformation gradient, $\mathbf{F}^*$, (including the elastic deformation and the rigid-body rotation), and a plastic deformation gradient, $\mathbf{F}^p$, Fig. 1, as follows:

$$\mathbf{F} = \mathbf{F}^* \mathbf{F}^p. \tag{1b}$$

By the polar decomposition theorem,

$$\mathbf{F}^* = \mathbf{V}^e \mathbf{R}^*, \tag{1c}$$

where $\mathbf{V}^e$ and $\mathbf{R}^*$ the left-stretch and the rigid-body rotation tensors, respectively, and superscripts e and $*$ stand for the elastic and non-plastic parts, respectively. The elastic left-stretch tensor is written as

$$\mathbf{V}^e = 1 + \boldsymbol{\varepsilon}, \tag{1d}$$

where $\boldsymbol{\varepsilon}$ is the strain measure in the rotated lattice.

The velocity gradient is

$$\mathbf{L} = \dot{\mathbf{F}}\mathbf{F}^{-1}, \tag{2a}$$

where dot stands for the time derivative. With the aid of (1b), $\mathbf{L}$ is divided into the non-plastic, $\mathbf{L}^*$, and plastic, $\mathbf{L}^p$ parts, as follows:

$$\mathbf{L} = \mathbf{L}^* + \mathbf{L}^p, \tag{2b}$$

$$\mathbf{L}^* = \dot{\mathbf{F}}^* \mathbf{F}^{*-1}, \tag{2c}$$

$$\mathbf{L}^p = \mathbf{F}^* \dot{\mathbf{F}}^p \mathbf{F}^{p-1} \mathbf{F}^{*-1}. \tag{2d}$$

In most situations, the major part of the crystal deformation is due to crystalline slip, with the accompanying elastic strain being very small. Hence, hereinafter, crystal kinematics with small elastic strains are discussed. Thus, by substituting (1c,d)

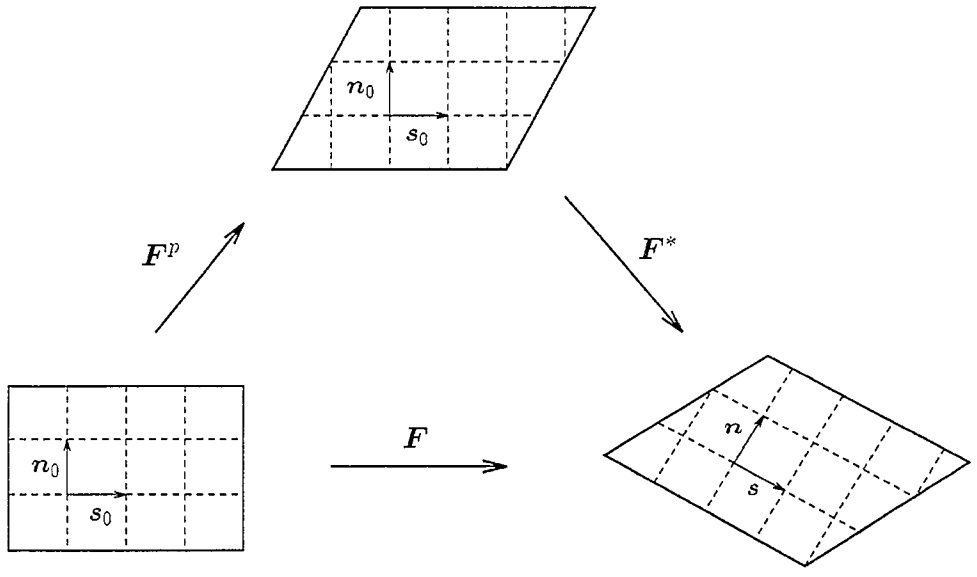

n_0 : initial slip plane normal

s_0 : initial slip direction

n : slip plane normal after deformation

s : slip direction after deformation

Fig. 1. Deformation of single crystal.

into (2c), the non-plastic velocity gradient is rewritten as

$$\mathbf{L}^* = \dot{\boldsymbol{\varepsilon}} + \boldsymbol{\varepsilon}\boldsymbol{\Omega}^* - \boldsymbol{\Omega}^*\boldsymbol{\varepsilon} + \boldsymbol{\Omega}^*, \tag{3a}$$

where the higher order terms in $\boldsymbol{\varepsilon}$ are neglected, and $\boldsymbol{\Omega}^*$ is the spin rate defined by

$$\boldsymbol{\Omega}^* = \dot{\mathbf{R}}^*\mathbf{R}^{*\mathrm{T}}. \tag{3b}$$

The symmetric and antisymmetric parts of $\mathbf{L}^*$ are the rate of lattice deformation, $\mathbf{D}^*$, and lattice spin, $\mathbf{W}^*$, respectively. These are given by

$$\mathbf{D}^* = \dot{\boldsymbol{\varepsilon}} + \boldsymbol{\varepsilon}\boldsymbol{\Omega}^* - \boldsymbol{\Omega}^*\boldsymbol{\varepsilon}, \tag{3c}$$

$$\mathbf{W}^* = \boldsymbol{\Omega}^*. \tag{3d}$$

In this work, the plastic deformation is assumed to be solely due to crystalline slip. The fcc single crystals have four slip planes and three slip directions on each slip plane. It, thus, follows that

$$\mathbf{L}^{\mathrm{p}} = \sum_{\alpha=1}^{4}\sum_{a=1}^{3} \dot{\gamma}^{(\alpha a)}\mathbf{l}^{(\alpha a)}, \tag{4a}$$

where $\dot{\gamma}^{(\alpha a)}$ is a slip rate and the slip system $\mathbf{l}^{(\alpha a)}$, is

$$\mathbf{l}^{(\alpha a)} = \mathbf{R}^*\mathbf{l}_0^{(\alpha a)}\mathbf{R}^{*\mathrm{T}}, \tag{5a}$$

$$\mathbf{l}_0^{(\alpha a)} = \mathbf{s}_0^{(\alpha a)} \otimes \mathbf{n}_0^{(\alpha)}. \tag{5b}$$

Here $\mathbf{n}_0$ and $\mathbf{s}_0$ are the unit normal of the slip plane and the unit vector in the slip direction, respectively. The subscript 0 stands for the initial configuration of the lattice and the superscript (αa) stands for the ath slip direction on the αth slip plane. The method of the numbering of the slip systems used in this work, is shown in Table 1. In this table the vectors in parentheses denote the slip plane normals and those in square blankets denote the slip directions. For future usage, the symmetric and antisymmetric parts of the slip system in the initial lattice configuration are expressed by $\mathbf{p}_0^{(\alpha a)}$ and $\mathbf{w}_0^{(\alpha a)}$, where

$$\mathbf{p}_0^{(\alpha a)} = \frac{1}{2}\left[\mathbf{l}_0^{(\alpha a)} + \mathbf{l}_0^{(\alpha a)^{\mathrm{T}}}\right], \tag{5c}$$

$$\mathbf{w}_0^{(\alpha a)} = \frac{1}{2}\left[\mathbf{l}_0^{(\alpha a)} - \mathbf{l}_0^{(\alpha a)^{\mathrm{T}}}\right]. \tag{5d}$$

Here the superscript T stands for the transpose.

The symmetric and antisymmetric parts of $\mathbf{L}^{\mathrm{p}}$ in (4a) are

$$\mathbf{D}^{\mathrm{p}} = \sum_{\alpha=1}^{4}\sum_{a=1}^{3} \dot{\gamma}^{(\alpha a)}\mathbf{p}^{(\alpha a)}, \tag{4b}$$

$$\mathbf{W}^{\mathrm{p}} = \sum_{\alpha=1}^{4}\sum_{a=1}^{3} \dot{\gamma}^{(\alpha a)}\mathbf{w}^{(\alpha a)}, \tag{4c}$$

where

$$\mathbf{p}^{(\alpha a)} = \mathbf{R}^*\mathbf{p}_0^{(\alpha a)}\mathbf{R}^{*\mathrm{T}}, \tag{5e}$$

$$\mathbf{w}^{(\alpha a)} = \mathbf{R}^*\mathbf{w}_0^{(\alpha a)}\mathbf{R}^{*\mathrm{T}}. \tag{5f}$$

From (3a–d), and (4a), Eq. (2b) becomes

$$\mathbf{L} = \mathbf{D}^* + \sum_{\alpha=1}^{4}\sum_{a=1}^{3} \dot{\gamma}^{(\alpha a)}\mathbf{l}^{(\alpha a)}. \tag{2e}$$

Symmetric and antisymmetric parts, then, become

$$\mathbf{D} = \mathbf{D}^* + \boldsymbol{\Omega}^* + \sum_{\alpha=1}^{4}\sum_{a=1}^{3} \dot{\gamma}^{(\alpha a)}\mathbf{p}^{(\alpha a)}, \tag{2f}$$

$$\mathbf{W} = \boldsymbol{\Omega}^* + \sum_{\alpha=1}^{4}\sum_{a=1}^{3} \dot{\gamma}^{(\alpha a)}\mathbf{w}^{(\alpha a)}. \tag{2g}$$

Table 1
Numbering of slip systems

(11)	$(111)[\bar{1}10]$
(12)	$(111)[0\bar{1}1]$
(13)	$(111)[10\bar{1}]$
(21)	$(\bar{1}11)[\bar{1}\bar{1}0]$
(22)	$(\bar{1}11)[101]$
(23)	$(\bar{1}11)[01\bar{1}]$
(31)	$(1\bar{1}1)[1\bar{1}0]$
(32)	$(1\bar{1}1)[011]$
(33)	$(1\bar{1}1)[\bar{1}0\bar{1}]$
(41)	$(11\bar{1})[110]$
(42)	$(11\bar{1})[\bar{1}01]$
(43)	$(11\bar{1})[0\bar{1}1]$

2.2. Constitutive relations

First, the elastic constitutive relation is considered. It is assumed in this work that the stress, $\boldsymbol{\sigma}$, is linearly related to the Lagrangian strain, $\mathbf{E} = \frac{1}{2}(\mathbf{F}^{\mathrm{T}}\mathbf{F} - \mathbf{1})$, in the unrotated lattice,

$$\mathbf{R}^{*\mathrm{T}}\boldsymbol{\sigma}\mathbf{R}^* = \mathbf{C}:\mathbf{E}, \tag{6}$$

where $\mathbf{C}$ is the elastic tensor in the unrotated lattice. This assumption is valid for small elastic strains, as is the case for many metals. Then, with the aid of (3c), the time derivative of (6) becomes

$$\overset{\nabla}{\boldsymbol{\sigma}} = \mathbf{C}^* : \mathbf{D}^* = \mathbf{C}^* : (\mathbf{D} - \mathbf{D}^p), \tag{7}$$

where $\overset{\nabla}{\boldsymbol{\sigma}}$ is the Jaumann rate of the Cauchy stress,

$$\overset{\nabla}{\boldsymbol{\sigma}} = \dot{\boldsymbol{\sigma}} - \boldsymbol{\Omega}^* \boldsymbol{\sigma} + \boldsymbol{\sigma} \boldsymbol{\Omega}^*. \tag{8}$$

Here $\mathbf{C}^*$ is the elastic tensor in the rotation lattice.

Next, the flow rule is considered. In the current work, the rate-dependent slip model with the power law is employed. The slip rate of the (αa)th slip system is assumed to be given by

$$\dot{\gamma}^{(\alpha a)} = \dot{\gamma}_0^{(\alpha a)} \operatorname{sgn}(\tau^{(\alpha a)}) \left| \frac{\tau^{(\alpha a)}}{\tau_Y^{(\alpha a)}} \right|^m, \tag{9a}$$

where $\tau^{(\alpha a)}$ is the resolved shear stress,

$$\tau^{(\alpha a)} = \langle \boldsymbol{\sigma}, \mathbf{p}^{(\alpha a)} \rangle, \tag{9b}$$

and

$$\operatorname{sgn}(x) = \begin{cases} 1 & \text{for } x \geq 0 \\ -1 & \text{for } x < 0. \end{cases} \tag{10}$$

In Eq. (9a), $\tau_Y^{(\alpha a)}$ and $\dot{\gamma}_0^{(\alpha a)}$ are the critical resolved shear stress and the reference value of the slip rate, respectively. A linear hardening is assumed and the rate of change of the critical resolved shear stress is expressed as

$$\dot{\tau}_Y^{(\alpha a)} = \sum_{\beta=1}^{4} \sum_{b=1}^{3} h_{(\beta b)}^{(\alpha a)} \left| \dot{\gamma}^{(\beta b)} \right|, \tag{9c}$$

where $h_{(\beta b)}^{(\alpha a)}$ is the hardening matrix.

3. Interdependency of resolved shear stresses in fcc single crystals

The symmetric tensors $\mathbf{p}_0^{(\alpha a)}$'s, satisfy

$$\mathbf{p}_0^{(\alpha 1)} + \mathbf{p}_0^{(\alpha 2)} + \mathbf{p}_0^{(\alpha 3)} = \mathbf{0}, \quad \alpha = 1, 2, 3, 4, \tag{11a–d}$$

since the slip direction vectors on the same plane satisfy

$$\mathbf{s}_0^{(\alpha 1)} + \mathbf{s}_0^{(\alpha 2)} + \mathbf{s}_0^{(\alpha 3)} = 0, \quad \alpha = 1, 2, 3, 4;$$

see Table 1 for the numbering method. Besides the four constraints (11a–d), three other geometrical restrictions exist for $\mathbf{p}_0^{(\alpha a)}$'s, i.e.,

$$-\mathbf{p}_0^{(11)} + \mathbf{p}_0^{(22)} + \mathbf{p}_0^{(43)} = \mathbf{0}, \tag{11e}$$

$$-\mathbf{p}_0^{(12)} - \mathbf{p}_0^{(33)} + \mathbf{p}_0^{(41)} = \mathbf{0}, \tag{11f}$$

$$\mathbf{p}_0^{(13)} - \mathbf{p}_0^{(21)} + \mathbf{p}_0^{(32)} = \mathbf{0}. \tag{11g}$$

Restrictions (11a–g) remain valid throughout the deformation, independently of the rigid-body rotation of the lattice. From (11a–g), it is seen that only five of the twelve $\mathbf{p}^{(\alpha a)}$'s are independent.

From (9b) and (11a–d), the interdependency of the resolved shear stresses is expressed by

$$\tau^{(\alpha 1)} + \tau^{(\alpha 2)} + \tau^{(\alpha 3)} = 0, \quad \alpha = 1, 2, 3, 4; \tag{12a ~ c}$$

i.e., the sum of the resolved shear stresses on the same plane is always zero. Similarly, from (9b) and (11e–g),

$$-\tau^{(11)} + \tau^{(22)} + \tau^{(43)} = 0, \tag{12d}$$

$$-\tau^{(12)} - \tau^{(33)} + \tau^{(41)} = 0, \tag{12e}$$

$$\tau^{(13)} - \tau^{(21)} + \tau^{(32)} = 0. \tag{12f}$$

4. Solution algorithm

Eqs. (2f,g), and (8) are solved incrementally to obtain the deformation and stress states over a time increment. The plastic flow caused by crystallographic slip is incompressible. Hence, the volumetric strain, if any, is only due to the elastic lattice deformation, which can be dealt with separately. Therefore, at present, attention is focused only on the deviatoric elastoplastic crystal deformation. The velocity gradient, $\mathbf{L}$, is assumed to be a given deviatoric tensor over each time increment. Also, to simplify the results, isotropic elasticity is assumed.

The inner product of $\mathbf{D}$ in (2f) with $\mathbf{p}^{(\alpha a)}$ is given by

$$\langle \mathbf{D}, \mathbf{p}^{(\alpha a)} \rangle = \langle \mathbf{D}^*, \mathbf{p}^{(\alpha a)} \rangle + \sum_{\beta=1}^{4} \sum_{b=1}^{3} \dot{\gamma}^{(\beta b)} H_{(\beta b)}^{(\alpha a)}, \tag{13a}$$

where

$$H_{(\beta b)}^{(\alpha a)} = \langle \mathbf{p}^{(\beta b)}, \mathbf{p}^{(\alpha a)} \rangle. \tag{14}$$

With the aid of (3b,c), (5e), (7), and (8), the time derivative of (9b) becomes

$$\dot{\tau}^{(\alpha a)} = 2\mu\langle \mathbf{D}^*, \mathbf{p}^{(\alpha a)}\rangle, \tag{15}$$

where μ is the shear modulus. Substitution of (15) into (13a) yields

$$\langle \mathbf{D}, \mathbf{p}^{(\alpha a)}\rangle = \frac{1}{2\mu}\dot{\tau}^{(\alpha a)} + \sum_{\beta=1}^{4}\sum_{b=1}^{3}\dot{\gamma}^{(\beta b)}\mathrm{H}^{(\alpha a)}_{(\beta b)}. \tag{13b}$$

For the active slip systems, $|\dot{\tau}^{(\alpha a)}|$ is very small in general, when m in (9a) is sufficiently large. Here, a slip system is called active if the absolute value of the resolved shear stress for that system is larger than its reference value, otherwise, the system is called non-active. The basic strategy of the proposed algorithm is to solve (13b) to obtain approximate slip rates of the active slip systems with the tentative assumption that the elastic contribution, $\dot{\tau}^{(\alpha a)}$, is zero (plastic-predictor). These slip rates are then modified to include the effect on the elastic contribution (elastic-corrector) in order to obtain the correct deformation and stress states.

Only five of the twelve $\mathbf{p}^{(\alpha a)}$'s are linearly independent, as shown in the Section 3. Therefore, in the absence of the $\dot{\tau}^{(\alpha a)}$-terms, the system of Eq. (13b)

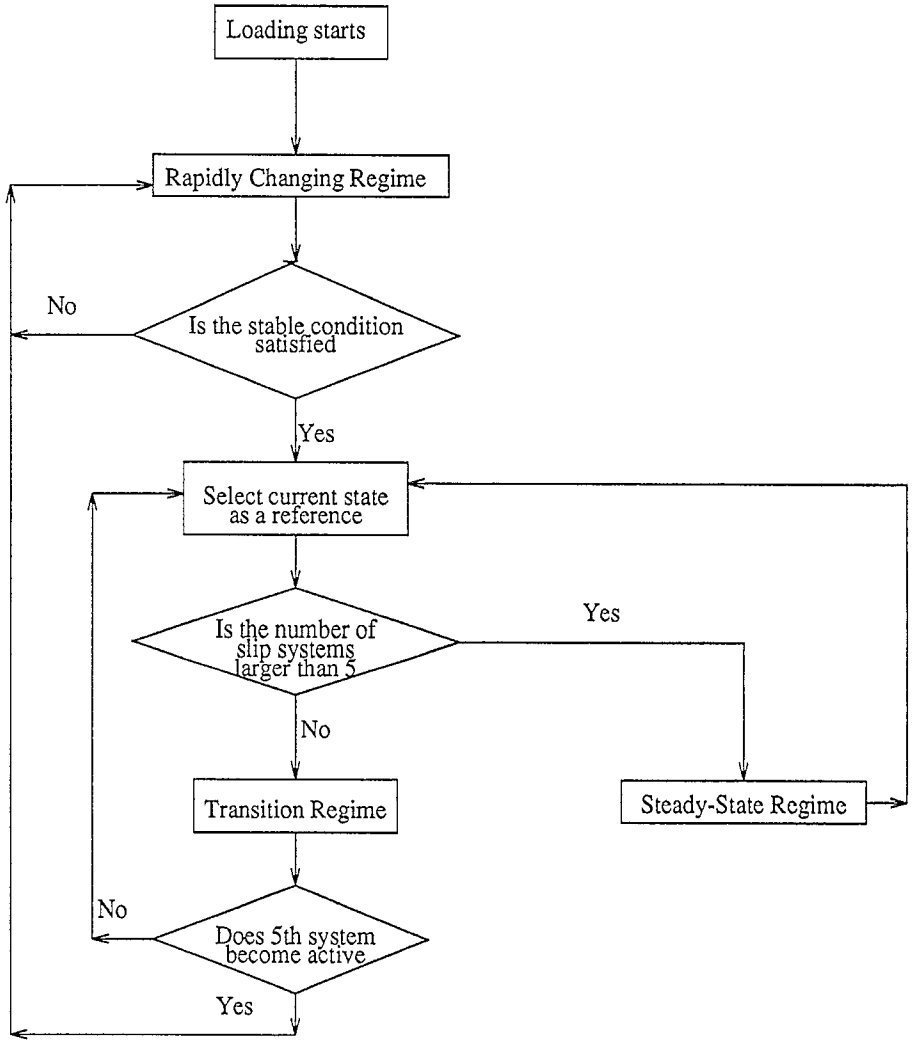

Fig. 2. Flow chart of the algorithm.

can't be solved to obtain more than five slip rates due to the singularity of the matrix **H**. Hence, if more than five slip systems are active, other conditions must be considered to supplement the number of equations. Therefore, different solution strategies are required depending on the number of the active slip systems.

The importance of the five independent slip systems is also shown from another viewpoint. It follows from Eq. (15) that $|\mathbf{D}^*| \approx 0$ is the necessary condition to satisfy $\dot{\tau}^{(\alpha a)} \approx 0$ in five independent slip systems. But, $|\mathbf{D}^*| \approx 0$ ensures $\dot{\tau}^{(\alpha a)} \approx 0$ in all slip systems. On the other hand, $\dot{\tau}^{(\alpha a)}$ for non-active slip systems may not be small in the case where less than five slip systems are active. For non-active slip systems, the resolved shear stresses may increase, and may render some of these systems active, when there are less than five active slip systems. For this reason, the deformation is called transitional in the case where less than five slip systems are active, and it is called steady if more than five slip systems are active. In general, less than five slip systems are active during the initial yielding, or when the loading is suddenly changed, and the number of active slip systems increases with time under a constant loading condition. In view of this observation, a material deformation history is divided into three regimes with respect to the number of active slip systems. These regimes are:

1. Transition regime: less than five slip systems are active.
2. Rapidly-changing regime: elastic deformation plays an important role.
3. Steady-state regime: more than five slip systems are active.

The rapidly changing regime connects the transition and steady-state regimes. In this regime, the elastic contribution plays an important role. The forward-gradient method is used to solve the rate equations in this regime. The forward gradient method is also applied when the loading starts and when the loading condition is changed, since the elastic contribution then has a significant effect.

The flow chart of the proposed algorithm is shown in Fig. 2. In this chart, the stable condition means that $\dot{\tau}^{(\alpha a)} \approx 0$ in all active slip systems. The plastic-predictor elastic-corrector algorithm is used in transition regime when the active slip systems are linearly independent, and in steady-state regime when five independent systems are active. If this is not the case, the forward-gradient method is applied. Although the plastic-predictor elastic-corrector algorithm is applicable, the forward-gradient method is preferred in such cases, since the search of the interdependency in the active slip systems becomes too complicated and hence, the algorithm becomes inefficient.

4.1. Transition regime

In this subsection, the case where less than five slip systems are active is discussed. Eq. (13b) is solved to obtain approximate slip rates of the active slip systems with the tentative assumption that the deformation is accompanied by no elastic distortion in the active slip systems, and that slip rates of non-active slip systems are zero. The resulting expressions are then corrected to include the elastic lattice deformation. It is also assumed that the increment of the rigid-body rotation in the concerned time step is sufficiently small, so that it can be approximated by

$$\Delta \mathbf{R}^* = \mathbf{1} + \mathbf{\Omega}^*_{(t_0)} \Delta t,$$

where t_0 marks the beginning of the time step, and Δt is the time increment. Then, $\mathbf{p}^{(\alpha a)}_{\mathrm{A}(t0+\Delta t)}$ is given by

$$\begin{aligned} \mathbf{p}^{(\alpha a)}_{\mathrm{A}(t_0+\Delta t)} &= \Delta \mathbf{R}^* \, \mathbf{p}^{(\alpha a)}_{(t_0)} \Delta \mathbf{R}^{*\mathrm{T}} \\ &\simeq \mathbf{p}^{(\alpha a)}_{(t_0)} + \mathbf{p}^{(\alpha a)}_{(t_0)} \mathbf{\Omega}^*_{(t_0)} \Delta t - \mathbf{\Omega}^*_{(t_0)} \mathbf{p}^{(\alpha a)}_{(t_0)} \Delta t, \end{aligned} \tag{16}$$

where the subscript A stands for the approximated value, since the lattice elastic strains and the variation in the spin during the time step are not yet included.

Then, Eq. (13b) is rewritten as

$$\langle \mathbf{D}, \mathbf{p}^{(\alpha a)}_{\mathrm{A}(t_0+\Delta t)} \rangle = \sum_{\beta} \sum_{b} \dot{\gamma}^{(\beta b)}_{\mathrm{A}} \mathrm{H}^{(\alpha a)}_{(\beta b)}, \tag{17a}$$

at time $t_0 + \Delta t$, where the summation is performed only on active slip systems, and $\dot{\gamma}^{(\alpha a)}_{\mathrm{A}}$ is the approximate value of the slip rate. Solving (17a), obtain

$$\dot{\gamma}^{(\alpha a)}_{\mathrm{A}} = \sum_{\beta} \sum_{b} \mathrm{K}^{(\beta b)}_{(\alpha a)} \langle \mathbf{D}, \mathbf{p}^{(\alpha a)}_{\mathrm{A}(t_0)} \rangle, \tag{17b}$$

where $\mathbf{K}$ is the inverse of a submatrix of $\mathbf{H}$, which corresponds to the active slip systems; the dimension of the involved submatrix of $\mathbf{H}$ correlates with the number of active slip systems. Since there are less than five active slip systems in this regime, and these are linearly independent, the submatrix of $\mathbf{H}$ is non-singular and $\mathbf{K}$ exists.

Express the inverse of (9a) as

$$\tau^{(\alpha a)} = \tau_{\mathrm{Y}}^{(\alpha a)} \operatorname{sgn}\left(\dot{\gamma}^{(\alpha a)}\right) \left| \frac{\dot{\gamma}^{(\alpha a)}}{\dot{\gamma}_0^{(\alpha a)}} \right|^{1/m}. \tag{18}$$

Substitute $\dot{\gamma}_{\mathrm{A}}^{(\alpha a)}$ into (9c) to obtain $\tau_{\mathrm{Y_A}}^{(\alpha a)}$. Then, substitute $\dot{\gamma}_{\mathrm{A}}^{(\alpha a)}$ and $\tau_{\mathrm{Y_A}}^{(\alpha a)}$ into (18) to obtain the approximate value of the resolved shear stress, $\tau_{\mathrm{A}}^{(\alpha a)}$.

Next the error due to neglecting the elastic contribution is estimated and corrected. The time integration of (13b) yields

$$\int_{t_0}^{t_0+\Delta t} \langle \mathbf{D}, \mathbf{p}^{(\alpha a)}(\xi) \rangle \, \mathrm{d}\xi = \frac{1}{2\mu} \Delta\tau^{(\alpha a)} + \sum_{\beta} \sum_{b} \Delta\gamma^{(\beta b)} \mathrm{H}_{(\beta b)}^{(\alpha a)}, \tag{19a}$$

where

$$\Delta\tau^{(\alpha a)} = \int_{t_0}^{t_0+\Delta t} \dot{\tau}^{(\alpha a)}(\xi) \, \mathrm{d}\xi, \tag{19b}$$

$$\Delta\gamma^{(\alpha a)} = \int_{t_0}^{t_0+\Delta t} \dot{\gamma}^{(\alpha a)}(\xi) \, \mathrm{d}\xi. \tag{19c}$$

On the other hand, the time integration of (17a) over a time step leads to

$$\int_{t_0}^{t_0+\Delta t} \langle \mathbf{D}, \mathbf{p}_{\mathrm{A}}^{(\alpha a)}(\xi) \rangle \, \mathrm{d}\xi = \sum_{\beta} \sum_{b} \Delta\gamma_{\mathrm{A}}^{(\beta b)} \mathrm{H}_{(\beta b)}^{(\alpha a)}, \tag{20a}$$

where

$$\Delta\gamma_{\mathrm{A}}^{(\alpha a)} \simeq \dot{\gamma}_{\mathrm{A}}^{(\alpha a)} \Delta t. \tag{20b}$$

It is assumed that $\mathbf{p}^{(\alpha a)}(t) \simeq \mathbf{p}_{\mathrm{A}}^{(\alpha a)}(t)$ over the time increment, and hence, from (19a) and (20a),

$$\frac{1}{2\mu} \tau_{\mathrm{er}}^{(\alpha a)} + \sum_{\beta} \sum_{b} \gamma_{\mathrm{er}}^{(\beta b)} \mathrm{H}_{(\beta b)}^{(\alpha a)} = -\frac{1}{2\mu} \Delta\tau_{\mathrm{A}}^{(\alpha a)}, \tag{21a}$$

where

$$\Delta\tau_{\mathrm{A}}^{(\alpha a)} = \tau_{\mathrm{A}}^{(\alpha a)} - \tau_{(t_0)}^{(\alpha a)}, \tag{21b}$$

$$\tau_{\mathrm{er}}^{(\alpha a)} = \tau_{\mathrm{A}}^{(\alpha a)} - \tau_{(t_0+\Delta t)}^{(\alpha a)}, \tag{21c}$$

and

$$\gamma_{\mathrm{er}}^{(\alpha a)} = \int_{t_0}^{t_0+\Delta t} \left(\dot{\gamma}_{\mathrm{A}}^{(\alpha a)} - \dot{\gamma}^{(\alpha a)}(\xi) \right) \mathrm{d}\xi = (1-\theta) \dot{\gamma}_{\mathrm{er}}^{(\alpha a)} \Delta t. \tag{21d}$$

Here the subscript er stands for the error terms which have been introduced by neglecting the elastic contribution, and θ is a proper interpolation parameter. The error terms are evaluated at time $t_0 + \Delta t$.

For sufficiently small error terms, (18) is linearized to obtain

$$\tau_{\mathrm{er}}^{(\alpha a)} = \sum_{\beta} \sum_{b} \left[\delta_{(\alpha a)}^{(\beta b)} \frac{\tau_{\mathrm{A}}^{(\beta b)}}{m \dot{\gamma}_{\mathrm{A}}^{(\beta b)}} + \operatorname{sgn}\left(\dot{\gamma}_{\mathrm{A}}^{(\beta b)}\right) \mathrm{h}_{(\alpha a)}^{(\beta b)} \frac{\tau_{\mathrm{A}}^{(\alpha a)}}{\tau_{\mathrm{Y_A}}^{(\alpha a)}} (1-\theta) \Delta t \right] \dot{\gamma}_{\mathrm{er}}^{(\beta b)}, \tag{22a}$$

where

$$\dot{\gamma}_{\mathrm{er}}^{(\alpha a)} = \dot{\gamma}_{\mathrm{A}}^{(\alpha a)} - \dot{\gamma}_{(t_0+\Delta t)}^{(\alpha a)}, \tag{22b}$$

and the delta function, $\delta_{(\alpha a)}^{(\beta b)}$, is given by

$$\delta_{(\alpha a)}^{(\beta b)} = \begin{cases} 1 & \alpha = \beta \text{ and } a = b \\ 0 & \text{otherwise.} \end{cases} \tag{23}$$

Substitution of (21d) and (22a) into (21a) yields

$$\sum_{\beta} \sum_{b} \mathrm{P}_{(\alpha a)}^{(\beta b)} \dot{\gamma}_{\mathrm{er}}^{(\beta b)} = \frac{1}{2\mu} \Delta\tau_{\mathrm{A}}^{(\alpha a)}, \tag{24a}$$

where

$$\mathrm{P}_{(\alpha a)}^{(\beta b)} = \frac{1}{2\mu} \left[\delta_{(\alpha a)}^{(\beta b)} \frac{\tau_{\mathrm{A}}^{(\beta b)}}{m \dot{\gamma}_{\mathrm{A}}^{(\beta b)}} + \operatorname{sgn}\left(\dot{\gamma}_{\mathrm{A}}^{(\beta b)}\right) \mathrm{h}_{(\alpha a)}^{(\beta b)} \frac{\tau_{\mathrm{A}}^{(\alpha a)}}{\tau_{\mathrm{Y_A}}^{(\alpha a)}} (1-\theta) \Delta t \right] - \mathrm{H}_{(\alpha a)}^{(\beta b)} (1-\theta) \Delta t. \tag{24b}$$

The dimension of the matrix $\mathbf{P}$ corresponds to the number of active slip systems. The error term, $\dot{\gamma}_{\mathrm{er}}^{(\alpha a)}$,

is calculated from (24a) and then substituted into (22b) to obtain the slip rate, $\dot{\gamma}^{(\alpha a)}_{(t_0+\Delta t)}$. Substitution of the slip rate, $\dot{\gamma}^{(\alpha a)}_{(t_0+\Delta t)}$, into (9c) and (18) gives $\tau^{(\alpha a)}_{Y(t_0+\Delta t)}$ and $\tau^{(\alpha a)}_{(t_0+\Delta t)}$, respectively.

The slip rate is also substituted into (2f,g) to obtain

$$\mathbf{D}^* = \mathbf{D} - \sum_{\alpha}\sum_{a} \dot{\gamma}^{(\alpha a)}_{(t_0+\Delta t)} \mathbf{p}^{(\alpha a)}_{A(t_0+\Delta t)}, \tag{25a}$$

and

$$\mathbf{\Omega}^* = \mathbf{W} - \sum_{\alpha}\sum_{a} \dot{\gamma}^{(\alpha a)}_{(t_0+\Delta t)} \mathbf{w}^{(\alpha a)}_{A(t_0+\Delta t)}, \tag{25b}$$

where $\mathbf{w}^{(\alpha a)}_{A}$ is obtained in the same manner as $\mathbf{p}^{(\alpha a)}_{A(t_0+\Delta t)}$. Here, it may be reasonable to assume constant non-plastic deformation and spin rates over a time increment. Hence, the Cayley–Hamilton theorem is applied to calculate the increment of the rigid-body rotation,

$$\Delta \mathbf{R}^* = 1 + \frac{\sin\omega}{\omega}\mathbf{\Omega}^*\Delta t + \frac{1-\cos\omega}{\omega^2}(\mathbf{\Omega}^*\Delta t)^2, \tag{26a}$$

where

$$\omega^2 = -\frac{\mathrm{tr}\left[(\mathbf{\Omega}^*\Delta t)^2\right]}{2}. \tag{26b}$$

Hence, the symmetric and antisymmetric parts of the slip system are updated by

$$\mathbf{p}^{(\alpha a)}_{(t_0+\Delta t)} = \Delta \mathbf{R}^*\, \mathbf{p}^{(\alpha a)}_{(t_0)} \Delta \mathbf{R}^{*\mathrm{T}}, \tag{27a}$$

and

$$\boldsymbol{\omega}^{(\alpha a)}_{(t_0+\Delta t)} = \Delta \mathbf{R}^* \boldsymbol{\omega}^{(\alpha a)}_{(t_0)} \Delta \mathbf{R}^{*\mathrm{T}}. \tag{27b}$$

From (25a) and (15),

$$\tau^{(\alpha a)}_{(t_0+\Delta t)} \approx \tau^{(\alpha a)}_{(t_0)} + \dot{\tau}_{(t_0+\Delta t)}\Delta t = \tau^{(\alpha a)}_{(t_0)} + 2\mu \times \left[\langle \mathbf{D}, \mathbf{p}^{(\alpha a)}_{(t_0+\Delta t)}\rangle - \sum_{\beta}\sum_{b} \dot{\gamma}^{(\beta b)}_{(t_0+\Delta t)} \mathrm{H}^{(\alpha a)}_{(\beta b)}\right]\Delta t. \tag{28}$$

The increment of the resolved shear stresses in non-active slip systems and the new slip systems which become active during the concerned time step, must be established. If the resolved shear stress in the currently non-active slip system satisfies

$$|\tau^{(\alpha a)}_{(t_0+\Delta t)}| \geq \tau^{(\alpha a)}_{Y(t_0+\Delta t)}, \tag{29}$$

then this system is said to have become active during this time increment. Since several slip systems may satisfy (29), the time increment $\Delta t_{(\alpha a)}$ which satisfies

$$|\tau^{(\alpha a)}_{(t_0)} + \dot{\tau}^{(\alpha a)}\Delta t_{(\alpha a)}| = \tau^{(\alpha a)}_{Y}, \tag{30}$$

is calculated for each slip system which satisfies (29). The smallest time increment, say, $\Delta t_{(\alpha a)}$, is then chosen. At $t_0 + \Delta t_{(\alpha a)}$, the effect of the new active slip systems must be included. Here, again, it is noted that the new active system need not be unique and more than one slip system may become active simultaneously. If the total number of active slip systems, including the new active slip systems, is less than five, then the deformation and stress states are calculated at time $t_0 + \Delta t_{(\alpha a)}$ and the next time step starts from this instant. On the other hand, if the number of active slip systems becomes larger than five, the rapidly-changing regime is attained, since the contribution of the elastic deformation plays an important role until the stable condition is satisfied for more than five active slip systems. The subsequent deformation and stress increments are calculated by the forward-gradient method in this regime.

4.2. Rapidly-changing regime

In this subsection, we consider the case where the elastic contribution plays an important role. The forward-gradient method is then used to solve the rate equations. This calculation technique is also applied at the initial loading, and when the loading condition is abruptly changed, since the elastic contribution then has a significant effect.

For sufficiently small time increment, the time integration of (13b) yields

$$\langle \mathbf{D}, \mathbf{p}^{(\alpha a)}_{(t_0)}\rangle \Delta t = \frac{1}{2\mu}\Delta\tau^{(\alpha a)} + \sum_{\beta}\sum_{b} \Delta\gamma^{(\beta b)} \mathrm{H}^{(\alpha a)}_{(\beta b)}, \tag{31}$$

where, again, t_0 marks the beginning of the time step, and Δt is the time increment. Over this time increment, the increment of slip rates is expected to be sufficiently small, and hence, Eq. (9a) is linearized to obtain

$$\dot{\gamma}^{(\alpha a)}_{(t_0+\Delta t)} - \dot{\gamma}^{(\alpha a)}_{(t_0)} = \frac{\dot{\gamma}^{(\alpha a)}_{(t_0)}}{\tau^{(\alpha a)}_{(t_0)}}\Delta\tau^{(\alpha a)} - \sum_{\beta=1}^{4}\sum_{b=1}^{3} \times \operatorname{sgn}\left(\gamma^{(\beta b)}_{(t_0)}\right) h^{(\beta b)}_{(\alpha a)} \frac{\dot{\gamma}^{(\alpha a)}_{(t_0)}}{\tau^{(\alpha a)}_{Y(t_0)}}\Delta\gamma^{(\beta b)}. \tag{32}$$

By introducing a proper interpolation parameter θ, $\Delta\gamma^{(\alpha a)}$ is given by

$$\Delta\gamma^{(\alpha a)} = \left(\theta\dot{\gamma}^{(\alpha a)}_{(t_0)} + (1-\theta)\dot{\gamma}^{(\alpha a)}_{(t_0+\Delta t)}\right)\Delta t, \tag{33}$$

and hence, (32) is written as

$$\dot{\gamma}^{(\alpha a)}_{(t_0+\Delta t)} = \sum_{\beta=1}^{4}\sum_{b=1}^{3} A^{(\beta b)}_{(\alpha a)}\Delta\tau^{(\beta b)} + d_{(\alpha a)}, \tag{34a}$$

where

$$A^{(\beta b)}_{(\alpha a)} = \frac{\dot{\gamma}^{(\beta b)}_{(t_0)}}{\tau^{(\beta b)}_{(t_0)}}\left(\mathbf{T}^{-1}\right)^{(\beta b)}_{(\alpha a)}, \tag{34b}$$

$$d_{(\alpha a)} = \sum_{\beta=1}^{4}\sum_{b=1}^{3}\sum_{\phi=1}^{4}\sum_{c=1}^{3}\left(\mathbf{T}^{-1}\right)^{(\beta b)}_{(\alpha a)} \times \left[\delta^{(\phi c)}_{(\beta b)} - \operatorname{sgn}\left(\gamma^{(\phi c)}_{(t_0)}\right) h^{(\phi c)}_{(\beta b)} \times \frac{\dot{\gamma}^{(\beta b)}_{(t_0)}}{\tau^{(\beta b)}_{Y(t_0)}}\theta\Delta t\right]\dot{\gamma}^{(\phi c)}_{(t_0)}, \tag{34c}$$

and

$$T^{(\beta b)}_{(\alpha a)} = \delta^{(\beta b)}_{(\alpha a)} - \operatorname{sgn}\left(\gamma^{(\beta b)}_{(t_0)}\right) h^{(\beta b)}_{(\alpha a)} \frac{\dot{\gamma}^{(\alpha a)}_{(t_0)}}{\tau^{(\alpha a)}_{Y(t_0)}}(1-\theta)\Delta t. \tag{34d}$$

Substitution of (33) and (34a) into (31) yields

$$\sum_{\beta=1}^{4}\sum_{b=1}^{3} \times \left[\frac{1}{2\mu}\delta^{(\beta b)}_{(\alpha a)} + (1-\theta)\Delta t\sum_{\phi=1}^{4}\sum_{c=1}^{3} H^{(\phi c)}_{(\alpha a)} A^{(\beta b)}_{(\phi c)}\right] \times \Delta\tau^{(\beta b)} = \langle \mathbf{D}, \mathbf{p}^{(\alpha a)}_{(t_0)}\rangle\Delta t - \sum_{\beta=1}^{4}\sum_{b=1}^{3} H^{(\beta b)}_{(\alpha a)} \times \left(\theta\dot{\gamma}^{(\beta b)}_{(t_0)} + (1-\theta)d_{(\beta b)}\right)\Delta t. \tag{35}$$

Eq. (35) is solved to obtain $\Delta\tau^{(\alpha a)}$'s. Slip rates, $\dot{\gamma}^{(\alpha a)}_{(t_0+\Delta t)}$, are calculated from (9a) and then, the rigid-body rotation is updated by (25b)–(27b).

This calculation is repeated until the stable condition

$$\dot{\tau}^{(\alpha a)} \simeq 0$$

is attained for all active slip systems. When this condition is satisfied, the transition or the steady-state regime is attained, depending on the number of active slip systems.

4.3. Steady-state regime

In this subsection, the case where more than five slip systems are active is discussed. Eq. (17a) is solved to obtain approximate values of the slip rates of active slip systems and then, the error due to neglecting the elastic contribution is estimated and corrected. However, because of the singularity of the matrix **H**, (17a) provides only five linearly independent equations although more than five slip rates are unknown. Hence, these equations are supplemented by the relations among the resolved shear stresses, given in (12a–g). It is assumed in this work that the power coefficient m is sufficiently large and that the reference yield stress $\tau^{(\alpha a)}_{Y}$ does not have large variations among slip systems. It is observed from (12a–d) that three slip systems on the same slip plane can't be active simultaneously. For this observation and (12a–g), it follows that the number of active slip systems in the steady-state regime is either six or eight. In the case where six slip systems are active, two slip systems are active on three slip planes, and, in the other case, two slip systems are active on four slip planes. Since this regime always follows the calculation of the rapidly-changing regime, the number and the combination of active slip systems are always known at the beginning of this regime. Based on this knowledge, (12a–g) are redefined to include only the active slip systems. As

a result, only one interdependency equation is required for the case of six active slip systems, and three equations are required for the case of eight active slip systems. These dependency equations are collectively written in the matrix form as

$$\sum_{\alpha}\sum_{a} \mathrm{M}_i^{(\alpha a)}\tau^{(\alpha a)} = 0, \tag{36}$$

where summation is performed only on active slip systems. The dimension of the matrix $\mathbf{M}$ is 1×6 in the case where six slip systems are active, and 3×8 in the other case.

The assumption $\dot{\tau}^{(\alpha a)}$, leads that the increment of the resolved shear stresses is zero and hence, that of the slip rate is sufficiently small. Hence, Eq. (18) is linearized to read the approximate increment of the resolved shear stress such as

$$\Delta\tau_{\mathrm{A}}^{(\alpha a)} = \frac{\tau_{(t_0)}^{(\alpha a)}}{m\dot{\gamma}_{(t_0)}^{(\alpha a)}}\Delta\dot{\gamma}_{\mathrm{A}}^{(\alpha a)} + \sum_{\beta}\sum_{b}\mathrm{sgn}\left(\dot{\gamma}_{(t_0)}^{(\beta b)}\right)\mathrm{h}_{(\alpha a)}^{(\beta b)} \times \frac{\tau_{(t_0)}^{(\alpha a)}}{\tau_{\mathrm{Y}(t_0)}^{(\alpha a)}}\Delta\gamma_{\mathrm{A}}^{(\beta b)}, \tag{37a}$$

where

$$\Delta\dot{\gamma}_{\mathrm{A}}^{(\alpha a)} = \dot{\gamma}_{\mathrm{A}}^{(\alpha a)} - \dot{\gamma}_{(t_0)}^{(\alpha a)}, \tag{37b}$$

$$\Delta\gamma_{\mathrm{A}}^{(\alpha a)} = \int_{t_0}^{t_0+\Delta t}\dot{\gamma}_{\mathrm{A}}^{(\alpha a)}(\xi)\,\mathrm{d}\xi = \left[\theta\dot{\gamma}_{(t_0)}^{(\alpha a)} + (1-\theta)\dot{\gamma}_{\mathrm{A}}^{(\alpha a)}\right]\Delta t, \tag{37c}$$

and $\Delta\tau_{\mathrm{A}}^{(\alpha a)}$ is defined in (21b). Since Eq. (36) is valid independently of the deformation, the approximate increment of the resolved shear stress, $\Delta\tau_{\mathrm{A}}^{(\alpha a)}$, also satisfies (36). Hence, (37a–c) are substituted into (36) to obtain

$$\sum_{\alpha}\sum_{a}\mathrm{Q}_i^{(\alpha a)}\dot{\gamma}_{\mathrm{A}}^{(\alpha a)} = a_i, \tag{38a}$$

where

$$\mathrm{Q}_i^{(\alpha a)} = \sum_{\beta}\sum_{b}\mathrm{M}_i^{(\beta b)}\left[\delta_{(\beta b)}^{(\alpha a)}\frac{\tau_{(t_0)}^{(\beta b)}}{m\dot{\gamma}_{(t_0)}^{(\beta b)}} + \mathrm{sgn}\left(\dot{\gamma}^{(\alpha a)}\right)\mathrm{h}_{(\beta b)}^{(\alpha a)}\frac{\tau_{(t_0)}^{(\beta b)}}{\tau_{\mathrm{Y}(t_0)}^{(\beta b)}}(1-\theta)\Delta t\right], \tag{38b}$$

$$a_i = \sum_{\alpha}\sum_{a}\mathrm{M}_i^{(\alpha a)}\left[\frac{1}{m}\tau_{(t_0)}^{(\alpha a)} - \sum_{\beta}\sum_{b}\mathrm{sgn}\left(\dot{\gamma}_{(t_0)}^{(\beta b)}\right)\mathrm{h}_{(\alpha a)}^{(\beta b)}\frac{\tau_{(t_0)}^{(\alpha a)}}{\tau_{\mathrm{Y}(t_0)}^{(\alpha a)}}\theta\Delta t\dot{\gamma}_{(t_0)}^{(\beta b)}\right], \tag{38c}$$

and again, summation is performed only on active slip systems. The dimension of $\mathbf{Q}$ is 3×8 in the case where eight slip systems are active and 1×6 in the case where six slip systems are active. Eq. (38a) is combined with (17a) to obtain the approximate slip rates, $\dot{\gamma}_{\mathrm{A}}^{(\alpha a)}$. The approximate reference values of the resolved shear stresses, $\tau_{\mathrm{Y_A}}^{(\alpha a)}$, and the approximate values of the resolved shear stresses, $\tau_{\mathrm{A}}^{(\alpha a)}$, are obtained from (9c) and (18), respectively.

Next, the error due to neglecting the elastic contribution is estimated and corrected. From (21c), (36) is rewritten as

$$\sum_{\alpha}\sum_{a}\mathrm{M}_i^{(\alpha a)}\tau_{(t_0+\Delta t)}^{(\alpha a)} = \sum_{\alpha}\sum_{a}\mathrm{M}_i^{(\alpha a)}\left(\tau_{\mathrm{A}}^{(\alpha a)} - \tau_{\mathrm{er}}^{(\alpha a)}\right) = 0. \tag{39}$$

Since the error term is assumed to be sufficiently small, (22a) is substituted into (39) to obtain

$$\sum_{\alpha}\sum_{a}\mathrm{S}_i^{(\alpha a)}\dot{\gamma}_{\mathrm{er}}^{(\alpha a)} = \mathrm{b}_i, \tag{40a}$$

where

$$\mathrm{S}_i^{(\alpha a)} = \sum_{\beta}\sum_{b}\mathrm{M}_i^{(\beta b)}\left[\delta_{(\beta b)}^{(\alpha a)}\frac{\tau_{\mathrm{A}}^{(\beta b)}}{m\dot{\gamma}_{a}^{(\beta b)}} + \mathrm{sgn}\left(\dot{\gamma}_{\mathrm{A}}^{(\alpha a)}\right)\mathrm{h}_{(\beta b)}^{(\alpha a)}\frac{\tau_{\mathrm{A}}^{(\beta b)}}{\tau_{\mathrm{Y_A}}^{(\beta b)}}(1-\theta)\Delta t\right], \tag{40b}$$

and

$$\mathrm{b}_i = \sum_{\alpha}\sum_{a}\mathrm{M}_i^{(\alpha a)}\tau_{\mathrm{A}}^{(\alpha a)}. \tag{40c}$$

Eq. (40a) is combined with (24a) to obtain $\dot{\gamma}_{\mathrm{er}}^{(\alpha a)}$'s. $\dot{\gamma}_{(t_0+\Delta t)}^{(\alpha a)}$ is calculated from (22b), and then substituted into (9c) and (18) to obtain $\tau_{\mathrm{Y}}^{(\alpha a)}$ and $\tau^{(\alpha a)}$, respectively. At the end, the rigid-body rotation is updated by (25b)–(27b).

5. Numerical examples and discussion

In order to examine the effectiveness of the proposed algorithm, three examples are considered. The results are compared with those obtained using the explicit Euler method with suitably large number of time steps, and the accuracy and the efficiency of the proposed algorithm are discussed. In these examples, the time increment is adjusted to allow 5% increment of the equivalent plastic strain in both the transition, and steady-state, regimes, while 0.02% increment of the equivalent strain is used for the forward-gradient method in the rapidly-changing regime. The numbering of the slip systems is shown in Table 1. The constitutive constants are: $m = 101$, $\tau_{Y_0} = 0.5$, $\mu = 200\tau_{Y_0}$, and $\dot{\gamma}_0 = 1.0\ s^{-1}$.

In example 1, the loading condition is

$$\mathbf{L} = \begin{bmatrix} 0 & 2000 & 0 \\ 2000 & 0 & 2000 \\ 0 & 2000 & 0 \end{bmatrix} (s^{-1}). \tag{41}$$

The calculated equivalent stress and slip rates are plotted in Figs. 3 and 4, respectively. In these figures, symbols represent the results of the proposed algorithm, while the solid lines are the results obtained by the explicit Euler method, using 8000 steps. The slip rates calculated by the explicit Euler method with 5500 steps are plotted in Fig. 5, in order

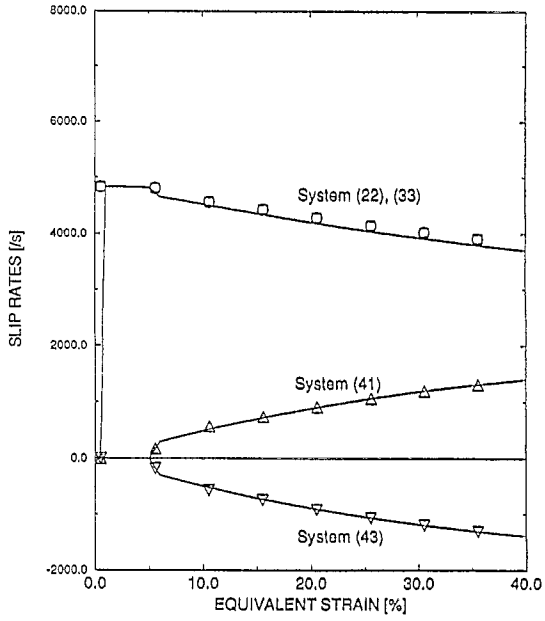

Fig. 4. Example 1: slip rates versus equivalent strain; symbols are given by the new algorithm, and the solid lines are given by the reference calculation.

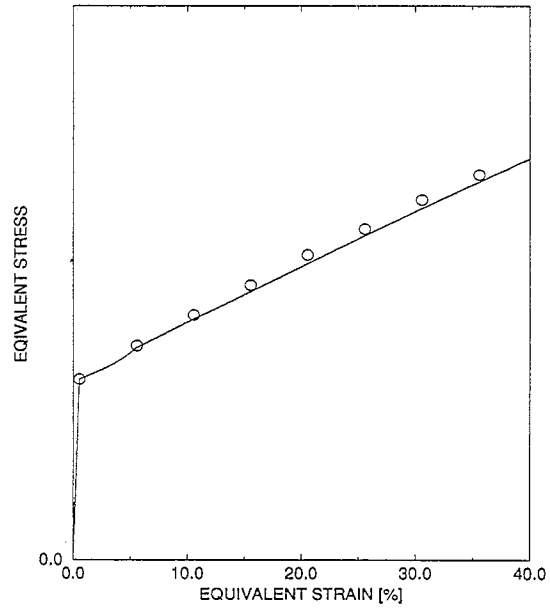

Fig. 3. Example 1: equivalent stress versus equivalent strain; the symbol is given by the new algorithm, and the solid line is given by the reference calculation.

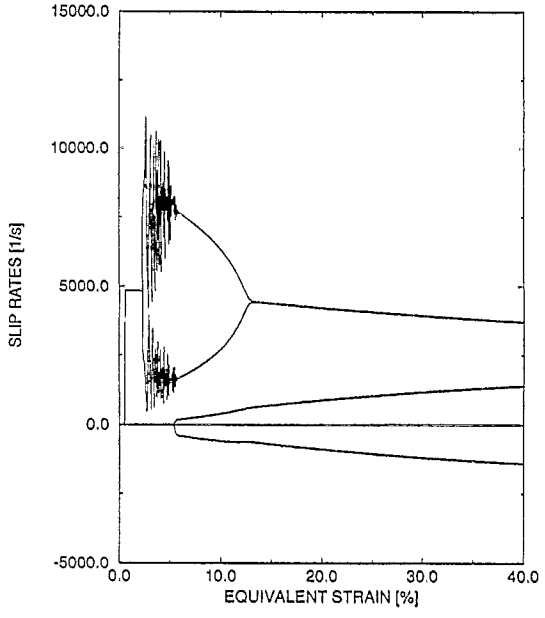

Fig. 5. Example 1: the explicit Euler method with 5500 steps. Calculated results are plotted at every 20 steps.

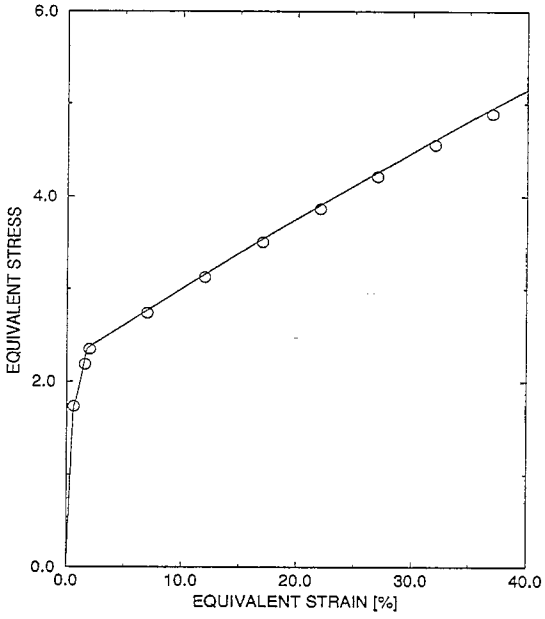

Fig. 6. Example 2: equivalent stress versus equivalent strain; the symbol is given by the new algorithm, and the solid line is given by the reference calculation.

to verify the number of time steps used in this example. Oscillation occurs due to the large time increment, and hence, it is concluded that 8000 steps are reasonable.

In this example, only four slip systems are active through the deformation and hence, the transition regime occurs for $0.56\% \leq \gamma_{eq}$, where γ_{eq} is the equivalent strain. The rapidly-changing regime occurs for $0\% \leq \gamma_{eq} < 0.56\%$. The steady-state regime does not appear. The proposed algorithm requires 0.43 CPU seconds on SPARC SUN workstation, while the reference calculation requires 8000 time steps with 7.19 CPU seconds.

The loading condition in example 2 is

$$\mathbf{L} = \begin{bmatrix} 0 & 2000 & 0 \\ 2000 & 0 & 4000 \\ 0 & 4000 & 0 \end{bmatrix} (s^{-1}). \tag{42}$$

The equivalent stress and slip rates are plotted in Figs. 6 and 7, respectively, to compare with the results of the explicit Euler method. In this example, the transition and steady-state regimes take place for $0.59\% \leq \gamma_{eq} < 1.55\%$ and $1.93\% \leq \gamma_{eq}$, respectively, and the rapidly-changing regime occurs for $0\% \leq \gamma_{eq} < 0.59\%$ and $1.55\% \leq \gamma_{eq} < 1.93\%$. The CPU time required for the new algorithm is 0.62 CPU seconds, while the Euler method requires 7.19 s with 8000 steps.

In example 3, the loading condition is changed in the middle of calculation as follows:

$$\mathbf{L} = \begin{bmatrix} 4000 & 0 & 0 \\ 0 & 4000 & 0 \\ 0 & 0 & -8000 \end{bmatrix} (s^{-1})$$

$$\text{for } 0 \leq \gamma_{eq} \leq 0.15, \tag{43}$$

$$\mathbf{L} = \begin{bmatrix} 0 & 2000 & 0 \\ 2000 & 0 & 0 \\ 0 & 0 & 0 \end{bmatrix} (s^{-1})$$

$$\text{for } 0.15 \leq \gamma_{eq} \leq 0.30. \tag{44}$$

The calculation results are plotted in Figs. 8 and 9, respectively. In Fig. 9, only slip rates on planes 1 and 2 are plotted, since slip rates on other plane show exactly the same behavior. It is noted that the rapidly-changing regime is attained at $\gamma_{eq} = 15\%$. The stability condition is satisfied for four active slip systems at $\gamma_{eq} = 15.07\%$. The proposed algorithm uses 0.6 CPU seconds, while the reference calculation requires 6000 steps with 13.86 CPU seconds.

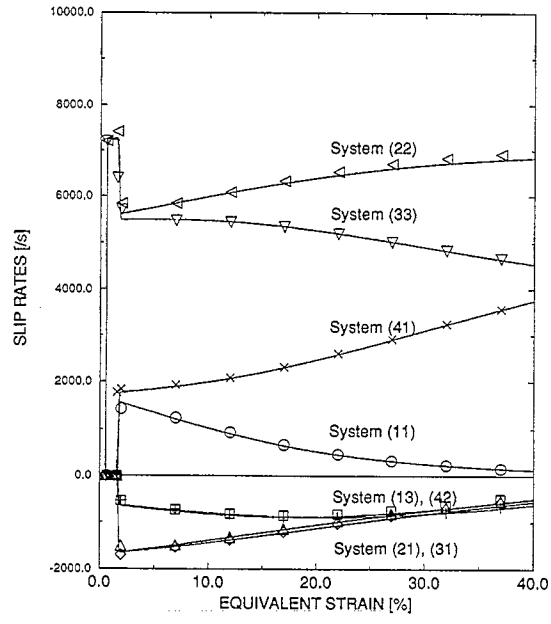

Fig. 7. Example 2: slip rates versus equivalent strain; symbols are given by the new algorithm, and the solid lines are given by the reference calculation.

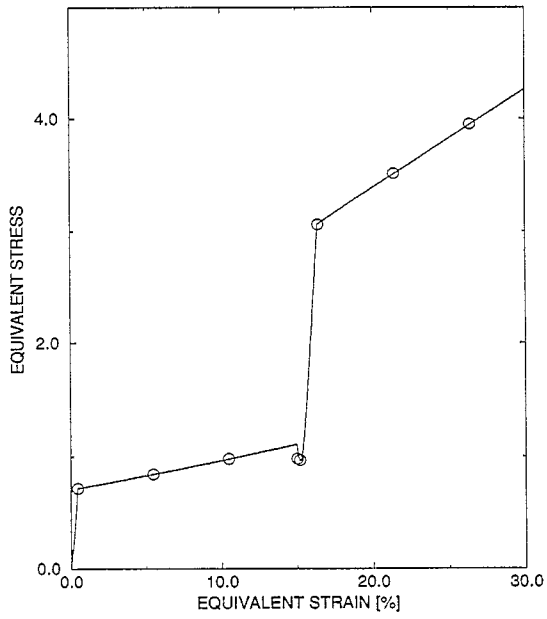

Fig. 8. Example 3: equivalent stress versus equivalent strain; the symbol is given by the new algorithm, and the solid line is given by the reference calculation.

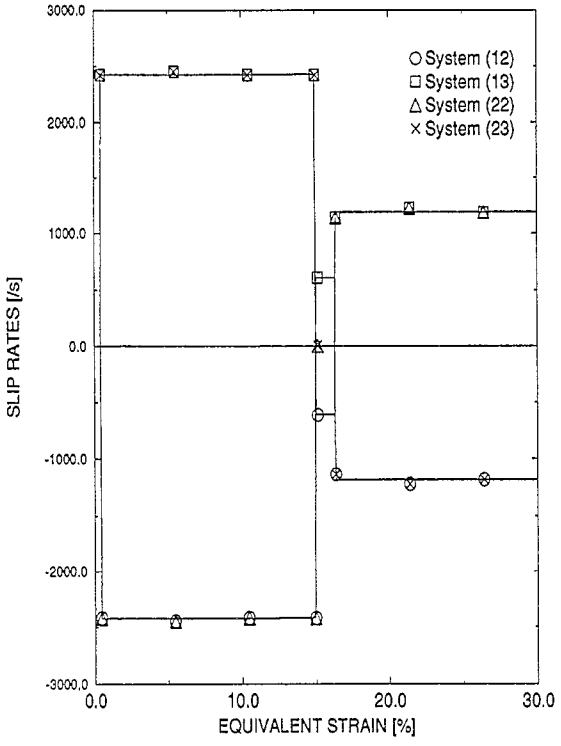

Fig. 9. Example 3: slip rates versus equivalent strain; symbols are given by the new algorithm, and the solid lines are given by the reference calculation.

In all examples, the results of the new algorithm show good agreement with the results of the Euler method which requires large number of time steps. The CPU time which is required for the proposed algorithm is less than 10% of that required for the Euler method. Although the proposed algorithm has more steps than the conventional forward-gradient method, it allows for much larger increment of the equivalent strain for the same accuracy. This results in considerable efficiency without sacrificing the required accuracy.

6. Conclusion

A new efficient algorithm is developed for an incremental calculation of finite deformation of fcc single crystals. The current configuration is selected as the reference one, and the increments of the deformation and stresses over a time increment, Δt, are calculated. The proposed algorithm combines the plastic-predictor elastic-corrector and the forward-gradient methods. When the elastic contribution is small compared to the plastic deformation, then an appropriate plastic-predictor elastic-corrector method is applied depending on the number of active slip systems, while the forward-gradient method is applied when the elastic contribution plays an important role. In the predictor–corrector method, first, the total deformation increment is assumed to be due to plastic flow (plastic-predictor), and then the results are corrected to account for the accompanying elastic deformation (elastic-corrector).

The accuracy and the efficiency of the algorithm proposed here are discussed through comparison of the results with those of the explicit Euler method. It is found that:

(1) The proposed algorithm for the fcc single crystals, has sufficient accuracy; and

(2) The proposed algorithm is much more efficient than the conventional method. The large time increment is successfully applied for predictor–corrector methods in the transition and steady-state regimes, where, respectively less than five, or more than five slip systems are active. Although the time increment used for the forward-gradient method in the rapidly-changing regime is as small as the one

for the reference calculation, this regime occurs over a relatively small time interval during the deformation history, compared to the transition and steady-state regimes where predictor–corrector methods are applied. Hence, the large time increment in the predictor–corrector methods results in much more efficient numerical scheme.

Acknowledgements

This research was supported by the Army Research Office under the contract number ARO DAAL 03-92-G-0108, and the National Science Foundations under the contract number MSS-90-21671 to the University of California, San Diego. The authors wish to thank ARO and NSF for supporting them throughout this study.

References

Asaro, R.J. (1979), Geometrical effects in the inhomogeneous deformation of ductile single crystals, *Acta Metall.* 27, 445.

Asaro, R.J. (1983), Crystal plasticity, *J. Appl. Phys.* 50, 921.

Asaro, R.J. and A. Needleman (1985), Texture development and strain hardening in rate dependent polycrystals, *Acta Metall.* 33, 923.

Balendran, B. and S. Nemat-Nasser (1994), Integration of inelastic constitutive equations for constant velocity gradient with large rotation, *Appl. Math. Comp.* 67, 161.

Havner, K.S. (1973), On the mechanics of crystalline solids, *J. Mech. Phys. Solids* 21, 383.

Havner, K.S. (1992), *Finite Plastic Deformation of Crystalline Solids*, Cambridge, New York.

Hill, R. (1966), Generalized constitutive relations for incremental deformation of metal crystals by multislip, *J. Mech. Phys. Solids* 14, 95.

Hill, R. and K.S. Havner (1982), Perspectives in the mechanics of elastoplastic crystal, *J. Mech. Phys. Solids* 30, 5.

Hutchinson, J.W. (1976), Bounds and self-consistent estimates for creep of polycrystalline materials, *Proc. R. Soc. London* A 348, 101.

Hill, R. and J.R. Rice (1972), Constitutive analysis of elastic–plastic crystals at arbitrary strain, *J. Mech. Phys. Solids* 20, 401.

Hutchinson, J.W. (1977), Creep and plasticity of hexagonal polycrystals as related to single crystal slip, *Metall. Trans.* 8A, 1465.

Iwakuma, T. and S. Nemat-Nasser (1984), Finite elastic plastic deformation of polycrystalline metals, *Proc. R. Soc. London* A394, 87.

Kroner, E. and C. Teodosiu (1974), Lattice defect approach to plasticity and viscoplasticity in problems of plasticity, in: ed. A, Sawczuk, *Symposium on Foundations of Plasticity*, Nordhoff International Pub., Leyden, p. 93.

Nemat-Nasser, S. (1983), On finite plastic flow of crystalline solids and geomaterials, *J. Appl. Mech.* 50, 1114.

Nemat-Nasser, S. (1991), Rate-independent finite-deformation elastoplasticity – a new explicit constitutive algorithm, *Mech. Mater.* 11, 235.

Nemat-Nasser, S. (1992), Phenomenological theories of elastoplastic and strain localization at high strain rates, *Appl. Mech. Rev.* 45, 19.

Nemat-Nasser, S. and D.T. Chung (1992), An explicit constitutive algorithm for large-strain, large-strain-rate elastic-viscoplasticity, *Comp. Meth. Appl. Mech. Eng.* 95, 205.

Nemat-Nasser, S. and Y.F. Li (1992), A new explicit algorithm for finite deformation elastoplasticity and elastoviscoplasticity: Performance evaluation, *Comp. Struct.* 44, 937.

Nemat-Nasser, S. and Y.F. Li (1994), An algorithm for large-scale computational finite-deformation plasticity, *Mech. Mater.* 18, 231.

Nemat-Nasser, S., M.M. Mehrabadi and T. Iwakuma (1981), On certain macroscopic and microscopic aspects of plastic flow of ductile materials, in: ed. S. Nemat-Nasser, *Three-Dimensional Constitutive Relations and Ductile Fracture*, North-Holland Publishing Company, North Holland, p. 157.

Nemat-Nasser S. and M. Obata (1986), Rate dependent, finite elasto–plastic deformation of polycrystal, *Proc. R. Soc. London* A407, 343.

Pan, J. and J.R. Rice (1983), Rate sensitivity of plastic flow and implications for yield surface vertices, *Int. J. Solids Struct.* 19, 973.

Peirce D., R.J. Asaro and A. Needleman (1983), Material rate dependence and localized deformation in crystalline solids, *Acta. Metall.* 31, 1951.

Rashid, M.M., G.T. Gray, III and S. Nemat-Nasser (1992), Heterogeneous deformation in copper single crystals at high and low strain rates, *Philos. Mag.* 65, 707.

Rashid and Nemat-Nasser (1990).

Rashid, M.M. and S. Nemat-Nasser (1992), A constitutive algorithm for rate-dependent crystal plasticity, *Comp. Meth. Appl. Mech. Eng.* 94, 201.

Rice, J.R. (1971), On the structure of stress–strain relations for time dependent plastic deformation in metals, *J. Appl. Mech.* 37, 728.

Rice, J.R. (1975), Continuum mechanics and thermodynamics of plasticity in relation to microscale deformation mechanisms, in: ed. A.S. Argom, *Equations in Plasticity*, MIT Press, Cambridge, p. 23.

Zikry, M.A. and S. Nemat-Nasser (1990), High-strain-rate localization and failure of crystalline materials, *Mech. Mater.* 10, 215.